The 9th European Congress on Computational Methods in Applied Sciences and Engineering
ECCOMAS Congress 2024
3–7 June 2024, Lisboa, Portugal

ON THE USAGE OF PANS FOR THE CFD SIMULATION OF WIND TURBINES

TIAGO GOMES[1], GUILHERME VAZ[1], ANTÓNIO MAXIMIANO[1], LUCIA SILEO[2] AND VLADIMIR KRASILNIKOV[2]

[1] blueOASIS (bO)
Rua do Norte 16, 2655-321 Ericeira, Portugal
e-mail: info@blueoasis.pt, www.blueoasis.pt

[2] SINTEF Ocean (SO)
Postboks 4762 Torgard, N-7465 Trondheim, Norway
email: ocean@sintef.no, www.sintef.no/en/ocean

Key words: Wind Turbines, Computational Fluid Dynamics (CFD), Partially Averaged Navier-Stokes (PANS), Reynolds Averaged Navier-Stokes (RANS), Delayed Dettached Eddy Simulation (DDES)

Summary. With the rapid evolution of offshore wind energy, engineering tools are crucial to catalyze technological developments and increase their maturity, therefore leading to lower costs. Complex turbine-turbine interactions require a good knowledge of the physics of the flow on, around and down/upstream of each turbine, which can be provided using high-fidelity CFD simulations. Turbulence models play a critical role on this matter and an adequate balance between accuracy and computational effort is necessary. While RANS approaches are quite efficient, LES should provide the most accurate result. Yet, even nowadays, LES blade-resolved simulations are still computationally prohibitive for industrial purposes. A middle-ground exists in SRS formulations, such as hybrid ones as DDES, or bridging ones such as PANS. In the present work emphasis is placed on PANS, since numerical and modelling errors can be studied and quantified independently, as opposite to other SRS approaches. Using as a benchmark the UNAFLOW wind turbine, it is found that traditional RANS and DDES turbulence formulations are able to predict integral forces, but partially fail in capturing wake mixing. Nevertheless, PANS, while enabling the user to select the ratio of turbulent quantities modelled, is not able to properly capture the integral forces due to premature separation in the blades. Several causes are discussed, including insufficient mesh refinement in the near-wall region and lack of turbulent content of the numerical inlet, preventing laminar to turbulent flow transition. Future work should focus on inlet synthetic turbulence generation, in line with existent literature, in order to improve the shortcomings faced in properly resolving the near-wall flow.

1 INTRODUCTION

Offshore wind energy is expected to become significantly relevant in the global renewable energy scenario, as floating technology evolves and unlocks more potential installation areas. As current floating wind farms develop from simple demonstrators, and commercial auctions lead to more floating wind farms worldwide, the technology needs to keep advancing to provide

better turbines that face the challenges of such installations, including complex turbine-turbine interactions. While Computational Fluid Dynamics (CFD) is arguably one of the best tools available to support that effort numerically, blade-resolved simulations remain too computationally intensive to be used regularly during an engineering project - in this case, more efficient mid- to low-fidelity tools tend to be preferred. Yet, CFD is able to provide very relevant insights into the physics of such flows, and therefore may be indispensable to support the development of such engineering tools. Indeed, the wake generated by the turbines is critical for their design, since it affects the loading and performance of the turbines immediately downstream. Furthermore, the fact that a floating turbine undergoes body-motions induced by the floating platform, further adds up to the complexity of the phenomena occurring in the wake. All of this requires appropriate turbulence mathematical approaches to be used, that find the appropriate trade-off between accuracy and computational effort.

Reynolds-Averaged Navier-Stokes (RANS) equations have been one of the most popular choices since they work with mean flow quantities and model the turbulence effects, thus alleviating the computational requirements [1, 2]. Yet, the fact that more general purpose closure models such as the two-equation $k-\epsilon$ tend to underperform (e.g. in capturing the wake recovery rate) led authors to devise corrections and alternative methods specific for wind turbine applications, including even data-driven approaches such as in [1]. On the opposite side of the spectrum are the Large Eddy Simulation (LES) formulations, that instead resolve most of the turbulent content of the flow, significantly contributing to a higher accuracy of the wake. Nevertheless, blade-resolved simulations using LES are still too computationally expensive due to the boundary layers, at high Reynolds numbers, requiring trade-offs in geometry capturing (e.g. using Actuator Disk or Actuator Line instead) or in the turbulence model itself [3]. In many engineering tools the turbine ends up just being modelled and is not included directly in the simulations, especially for cases with turbine-turbine interactions in wind farms.

Another alternative for wind energy high-fidelity blade-resolved simulations lies in hybrid RANS-LES methodologies, despite shortcomings identified in the work of [4]. These include Detached Eddy Simulation (DES) and its variations, as applied in [3], or Partially-Averaged Navier-Stokes (PANS) [5]. To the best knowledge of the authors, there is no open literature in which PANS is applied to wind turbine CFD simulations. Based on this premise, the present work will explore its usage for such application and compare it with other more traditional turbulence approaches. In Section 2 the mathematical formulation of each turbulence approach is presented, followed by an overview of the UNAFLOW wind turbine benchmark in Section 3. Then, in Section 4 the numerical setup of the CFD simulations are introduced, whereas in Section 5 and 6 the results obtained are discussed, followed by conclusions in Section 7.

2 TURBULENCE APPROACHES

2.1 Direct Numerical Simulation (DNS) and Large-Eddy Simulation (LES)

A viscous flow is governed by the Navier-Stokes equations, which at its basic incompressible unsteady form are composed by a mass conservation equation and a momentum balance equation,

$$\frac{\partial u_i}{\partial x_i} = 0 \quad ; \quad \frac{\partial u_i}{\partial t} + u_j \frac{\partial u_i}{\partial x_j} = -\frac{1}{\rho}\frac{\partial p}{\partial x_i} + \nu \frac{\partial^2 u_i}{\partial x_j x_j}. \tag{1}$$

Such set of equations only have analytical solution in a very restrict subset of cases, therefore requiring to be solved numerically which is the goal of Computational Fluid Dynamics (CFD). Nevertheless, the Direct Numerical Simulation (DNS) of these equations is not suitable for most cases of interest in which turbulent flow exists. Indeed, for high Reynolds numbers, part of the scales of the turbulent eddies become so small, that a very fine grid is necessary to properly resolve them. Even nowadays, the computational power available still dictates that DNS of turbulent flows for most mid to high-Reynolds numbers are still intractable [6].

An alternative formulation is the Large Eddy Simulation (LES), that takes advantage of the isotropic properties of the smallest dissipative turbulent scales to model them, resolving only the largest coherent structures. While alleviating the grid refinement requirements, it is still sometimes prohibitively expensive, especially for wall-bounded flows.

2.2 Reynolds-Averaged Navier-Stokes (RANS)

In order to circumvent the computational limitations of DNS and LES, the Reynolds-Averaged Navier-Stokes (RANS) equations assume that the flow is statistically steady, thus the instantaneous turbulent fluctuations can be decomposed in a ensemble, $\overline{\phi_i}$, and fluctuating part, ϕ_i', also known as Reyndolds decomposition, $\phi_i(x_i,t) = \overline{\phi_i}(x_i) + \phi_i'(x_i,t)$. Considering that the mean flow can also have a time dependency in unsteady flows, $\overline{\phi_i}(x_i,t)$, substituting it in the Navier-Stokes equations one obtains the unsteady RANS equations (URANS),

$$\frac{\partial \overline{u_i}}{\partial x_i} = 0 \quad ; \quad \frac{\partial \overline{u_i}}{\partial t} + \overline{u_j}\frac{\partial \overline{u_i}}{\partial x_j} = -\frac{1}{\rho}\frac{\partial \overline{p}}{\partial x_i} + \nu \frac{\partial^2 \overline{u_i}}{\partial x_j x_j} - \frac{\partial R_{ij}}{\partial x_j}, \tag{2}$$

in which a new non-linear term arises, $R_{ij} = \overline{u_i' u_j'}$, also known as Reynolds stress, that depends on the fluctuating part, introducing a closure problem. The Bousinesq approximation tackles this through the concept of eddy viscosity, an additional viscosity term proportional to the mean strain rate that models the effect of the turbulent stresses in the mean flow,

$$R_{ij} = -\nu_t \left(\frac{\partial \overline{u_i}}{\partial x_j} + \frac{\overline{u_j}}{\partial x_i} \right) + \frac{2}{3} k \delta_{ij}. \tag{3}$$

Such hypothesis enables turbulence closure models to be derived, such as the popular 2-equation $k-\omega$ SST [7] which spatially blends the $k-\epsilon$ and $k-\omega$ models according to their specific advantages,

$$\frac{\partial k}{\partial t} + \frac{\partial (k\overline{u_j})}{\partial x_j} = P_k - \beta^* k\omega + \frac{\partial}{\partial x_j}\left[(\nu + \nu_t \sigma_k) \frac{\partial k}{\partial x_j} \right] \tag{4}$$

$$\frac{\partial \omega}{\partial t} + \frac{\partial (\omega\overline{u_j})}{\partial x_j} = \frac{\alpha}{\nu_t} P_k - \beta\omega^2 + \frac{\partial}{\partial x_j}\left[(\nu + \nu_t \sigma_\omega) \frac{\partial \omega}{\partial x_j} \right] + \frac{2\sigma_{\omega_2}}{\omega}(1-F_1)\frac{\partial \omega}{\partial x_j}\frac{\partial k}{\partial x_j}. \tag{5}$$

More details regarding the meaning of each term and the values of the constants can be found in [7], which have been derived from experiments. Effectively, the RANS equations are based on the average flow, modelling all turbulence fluctuations through the means of the turbulence closure model. While this significantly reduces the grid refinement requirements compared with DNS and LES, it also brings the limitation that each closure model is in principle specifically crafted after an experimental flow, which limits its validity region.

2.3 Delayed Detached Eddy Simulation (DDES)

The Delayed Detached Eddy Simulation (DDES) [8] is an hybrid turbulence formulation, a variation of the original Detached Eddy Simulation (DES) that mixes different turbulence approaches: RANS in the attached boundary layer region and a Scale-Resolving Simulation (SRS) formulation in the outer and detached regions, in this case LES, where the grid resolution is expected to be more suitable for the local turbulent length scales. Assuming that the RANS closure model used is the $k-\omega$ SST [7], the k equation is modified to

$$\frac{\partial k}{\partial t}+\frac{\partial(k\overline{u_j})}{\partial x_j}=P_k-\frac{k^{\frac{3}{2}}}{l_{DDES}}+\frac{\partial}{\partial x_j}\left[(\nu+\nu_t\sigma_k)\frac{\partial k}{\partial x_j}\right] \tag{6}$$

where $l_{DDES}=l_{RANS}-f_d\max(0,l_{RANS}-l_{LES})$. Moreover, $l_{RANS}=\frac{\sqrt{k}}{C_{\mu\omega}}$ and $l_{LES}=C_{DES}h_{max}$, where h_{max} is the maximum cell size, indicating the dependence with grid refinement. More information about the value of the constants and the formula for the blending function f_d can be found in [8]. Note that this shielding function f_d is an improvement in relation to the original DES model, preventing premature transition from RANS to LES near the wall, which in some cases could lead to Grid Induced Separation (GIS) due to the sudden reduction of eddy viscosity, since the modelled turbulence stresses were not transferred to the LES region (Modelled Stress Depletion, MSD) [8]. With this, the outer flow can be more accurately resolved if enough grid refinement is provided, while keeping the cell count low in the near-wall region by using RANS to model the turbulent scales.

2.4 Partially Averaged Navier-Stokes (PANS)

Finally, the Partially Averaged Navier-Stokes (PANS) equations [5] are a bridging turbulence mathematical model, in a sense that it uses the same formulation across the domain. This approach adopts a filter that dictates the ratio of turbulent quantities being modelled, $f_\phi=\phi/\Phi$, where Φ represents a quantity and ϕ the modelled part. For the $k-\omega$ SST closure model [9], the original RANS equations are modified to

$$\frac{\partial k}{\partial t}+\frac{\partial(k\overline{u_j})}{\partial x_j}=P_k-\beta^*k\omega+\frac{\partial}{\partial x_j}\left[(\nu+\nu_t\sigma_k\frac{f_\omega}{f_k})\frac{\partial k}{\partial x_j}\right] \tag{7}$$

$$\frac{\partial \omega}{\partial t}+\frac{\partial(\omega\overline{u_j})}{\partial x_j}=\frac{\alpha}{\nu_t}P_k-\left(P'-\frac{P'}{f_\omega}+\frac{\beta\omega}{f_\omega}\right)\omega+\frac{\partial}{\partial x_j}\left[(\nu+\nu_t\sigma_\omega\frac{f_\omega}{f_k})\frac{\partial \omega}{\partial x_j}\right]+\frac{2\sigma_{\omega_2}}{\omega}\frac{f_\omega}{f_k}(1-F_1)\frac{\partial \omega}{\partial x_j}\frac{\partial k}{\partial x_j}, \tag{8}$$

where $P'=\frac{\alpha\beta^*k}{\nu_t}$ and $0.0\leq f_k\leq f_\omega\leq 1.0$, since the largest scales contain most of the kinetic energy and in the smallest scales is where dissipation occurs [5]. In this paper the PANS formulation assumes a spatially constant f_k and a f_ω equal to unity, which translates into all dissipation occuring in the modelled scales. It is argued that such formulation has the advantage of decoupling modelling and numerical errors, benefiting Verification exercises, and avoiding MSD at the interfaces of RANS-SRS in formulations such as DDES [10]. However, it can be challenging for practical cases to select a value for f_k [10]. In [11] the authors propose the

following equation to estimate the minimum f_k supported by the grid,

$$f_k \geq \frac{1}{C_\mu} \left(\frac{\Delta}{\Lambda} \right)^{\frac{2}{3}} \tag{9}$$

in which Δ is the smallest grid dimension and Λ the turbulent Taylor length scale, whose spatial distribution is recommended to be extracted from a preliminary RANS simulation.

3 UNAFLOW TEST CASE

The UNAFLOW test case [12] is used as a benchmark. It consists of a series of wind tunnel tests performed in the wind tunnel of Politecnico di Milano (PoliMi) using a modified model-scale DTU10MW wind turbine. The dataset includes integral forces and wake velocities, enabling Validation exercises to be performed. While one of its goals was to assess the capacity of different numerical methods to model correctly the aerodynamics of the turbine under imposed motion conditions, only the fixed case results are used in the present work. The experimental setup is shown in Figure 1, whereas in Table 1 some characteristics are provided.

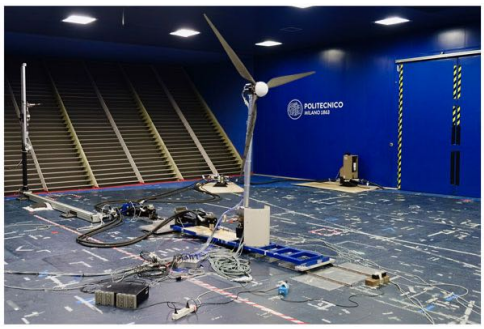

Figure 1: UNAFLOW experimental setup. Extracted from [12].

Table 1: UNAFLOW experiment characteristics.

General Dimensions	
Tunnel [LxWxH]	13.84 x 3.84 x 35.00 m
Turbine Diameter [D]	2.38 m
Operating Conditions	
Density [ρ]	1.177 kg/m^3
Dynamic Viscosity [μ]	1.84E-5 $Pa \cdot s$
Inlet Velocity [U_∞]	4.0 m/s
Turbulence Intensity [TI]	2.0 %
Angular Velocity [ω_{rotor}]	240 RPM

4 NUMERICAL SETUP

The UNAFLOW experimental setup, including both the wind tunnel and wind turbine geometries, were included in the computational domain as in Figure 2. The turbine geometry was obtained from the authors of [12], which required a few simplifications in the apparatus of the hub region to make it more suitable for CFD. On the other hand, the geometry of the floor shield is an approximation based on the pictures, since information about it could not be found.

The CFD solver used to perform these blade-resolved simulations is ReFRESCO [13] version 2023.1.0. This incompressible solver is based on unstructured grids, adopting a Finite Volume discretization approach with cell-centered collocated variables. Some of its features, used in the present work, include a wide range of turbulence formulations (e.g. RANS, LES and SRS) and capacity to include body-motions through the usage of Sliding Grids (SG). In this specific case, SG are used to incorporate the motion of the rotor, which is independently meshed from the rest of the domain. Both domains share an interface, where information is transferred through the means of an interpolation scheme - in this case using Least Square with a second-degree polynomial, which is third-order accurate.

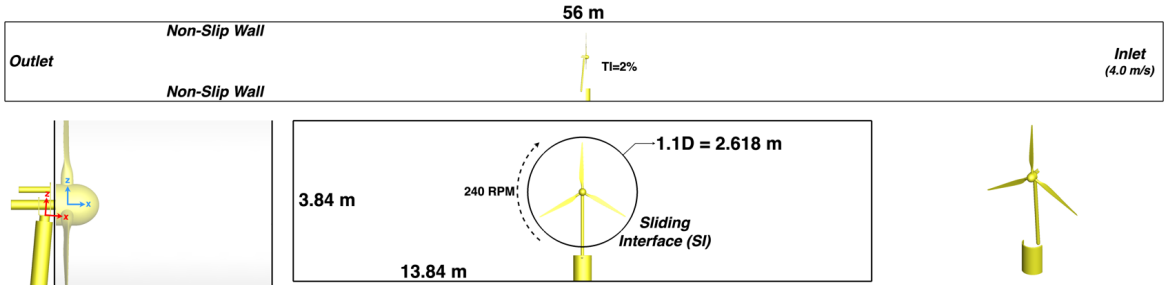

Figure 2: Computational domain of the UNAFLOW test case.

For time discretization an Implicit Three Time Level scheme is used, which is second-order accurate. For the momentum equation, a Total Variation Diminishing (TVD) Harmonic scheme is used, which is second-order accurate, whereas for the turbulence transport equations a first-order upwind scheme is adopted. All boundary layers are resolved by ensuring that $y^+ \approx 1.0$, with the only exception being in the tunnel walls where the target y^+ is 100.0 to apply wall functions instead.

Based on these considerations, three meshes were generated to perform Verification and Validation (V&V) studies. More information about them can be found in Table 2, including a slice of grid G3 in Figure 3. Here it is possible to observe the wake refinement, since it is one of the main components to be analyzed in the present study. In fact, a driving factor in generating these grids was the cell size in that region, which can be found in rotor diameter units also in Table 2.

Table 2: Grids.

Grid	h_i	N_{cells}	Δx_{wake}
G1	1.527	16.7M	$1.000\%D$
G2	1.395	21.9M	$0.750\%D$
G3	1.000	59.5M	$0.500\%D$

All simulations are unsteady and use a timestep based on the angular displacement of the rotor, ensuring that the Courant number is less than unity in most of the wake. A reference timestep of 3 degrees was set for grid G2, which was adapted for grid G1 (4 degrees) and grid G3 (2 degrees) based on the ratio of the cell size in the wake, in an attempt to keep the Courant number constant. Within each timestep 75 non-linear iterations of the equations are performed, which are found to reduce the L_2 norm of the residuals below 10^{-4}.

5 RANS AND DDES RESULTS

The first two turbulence formulations tested are RANS and DDES, both of which can find applications to wind turbines in the literature. Each simulation is executed for 20 rotor revolutions and the average of relevant quantities extracted using pyTST [14] based on the Transient Scanning Technique. All averaged quantities obtained have a 95% uncertainty associated that is at least two orders of magnitude lower than the average. In Figure 5 the result of the V&V exercise based on the theory of [15] is presented, with some recent still to be published variations and forcing a second-order fit based on the order of the discretization schemes used.

While the usage of a fourth grid refinement would be ideal, the current results show that a second order curve-fitting of the thrust and torque data points versus grid refinement has a relatively low uncertainty associated and approaches reasonably well the experimental results in the limit of infinitesimal grid cell size, where discretization error is negligible. In this limit,

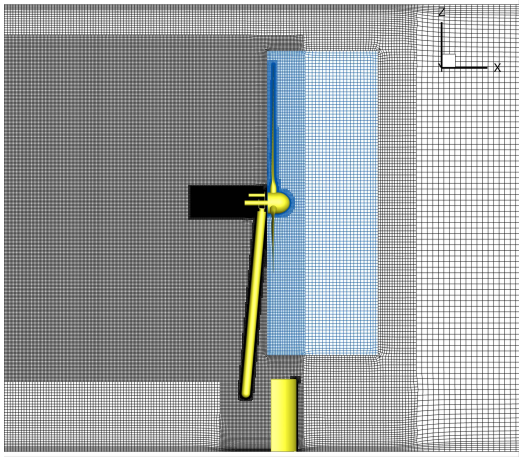

Figure 3: Slice of grid G3. In blue its rotating domain of rotor.

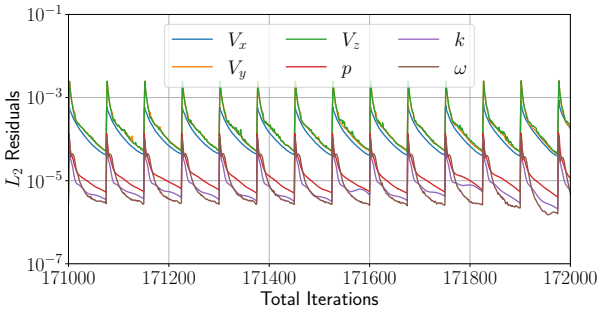

Figure 4: Residuals of grid G1 using the RANS turbulence model.

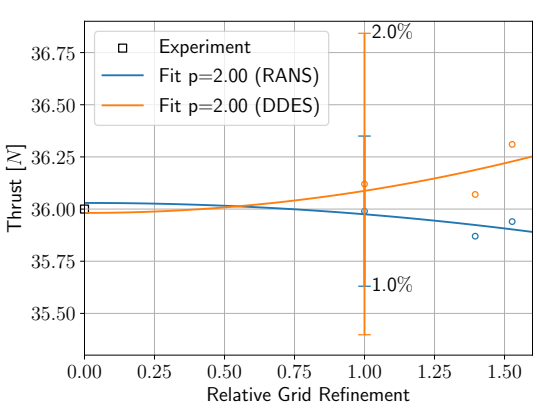

(a) Thrust [N]

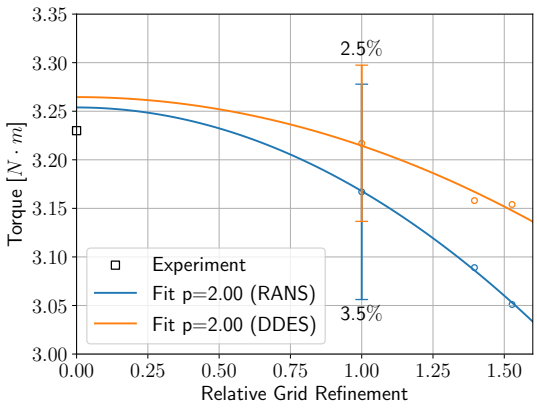

(b) Torque [$N \cdot m$]

Figure 5: V&V grid refinement study for RANS and DDES turbulence models.

only other error sources should exist, such as modelling errors from the turbulence formulations adopted. It is important also to note that UNAFLOW doesn't provide any kind of uncertainty quantification of the experiments.

Another output of UNAFLOW concerns the wake velocities using hot-wire measurements, which were measured for 1 minute, corresponding to 240 revolutions of the rotor. The cross-wire's data, which was placed $2.3D$ downstream, was time-averaged in order to obtain a single velocity profile, which is a good indicator of the wake momentum deficit introduced by the rotor. Considering that far less rotations were simulated, and that the first ones may be affected by transient numerical effects, only the last 5 rotations of each simulation are used to extract a similar average. The results can be analysed in Figure 6.

Overall, the momentum deficit at mid-radius imprinted by the blades is reasonably well captured by both turbulence formulations, despite some differences in the right side of the plot. Note that a similar result was observed in [16] using the same numerical setup but with a

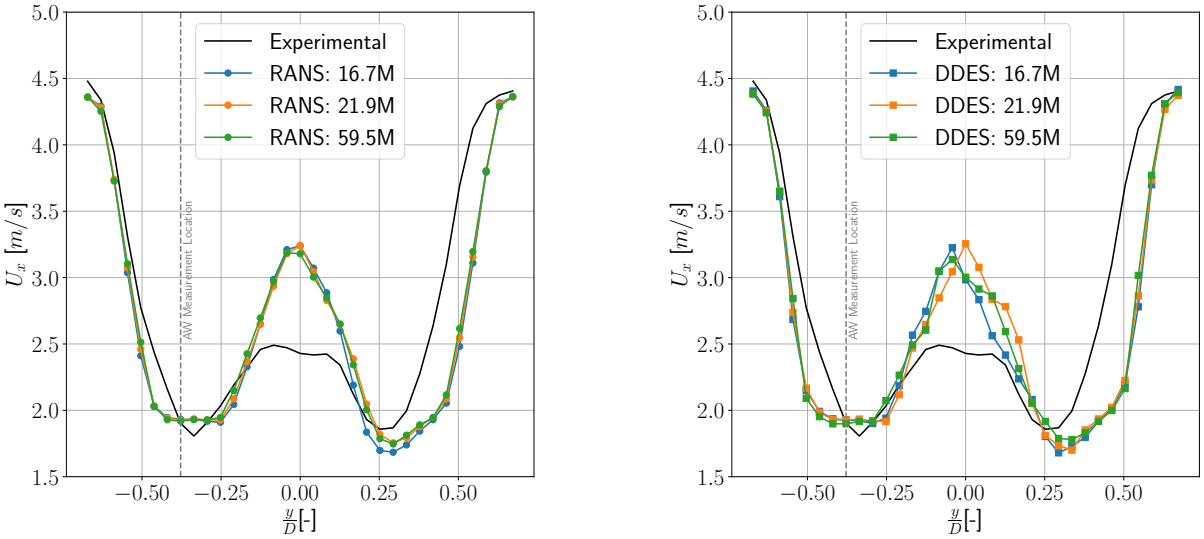

(a) RANS (b) DDES

Figure 6: Average cross-wire velocity measurements $2.3D$ downstream.

different CFD solver and settings.

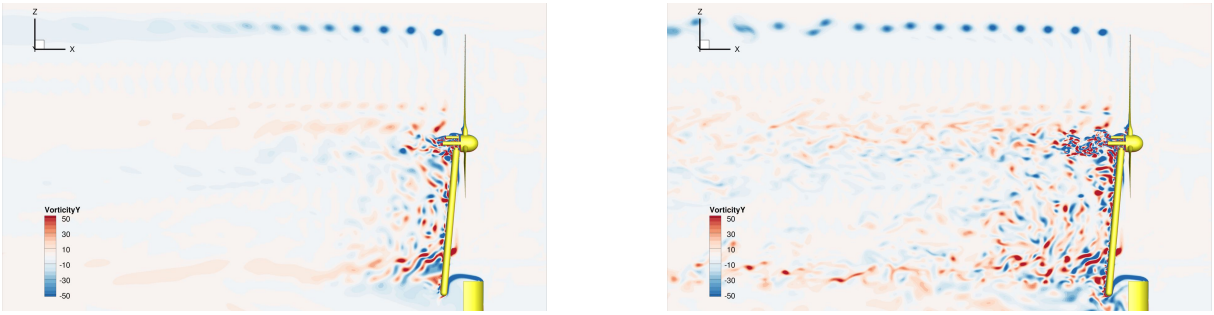

(a) RANS (b) DDES

Figure 7: Vorticity [s^{-1}] magnitude in y-axis at y=0 for grid G3.

However, the most significant differences occur at the center, where the flow is more energetic in the simulations than in the experiments. It is known that wind turbine wakes tend to have much more energetic cores, yet the shear stresses created by the less energetic fluid surrounding it induces turbulent mixing effects that smooths out that difference as it progresses downstream. Therefore, this difference may be an indication that both turbulence formulations fail to capture that mixing, either due to modelling limitations (RANS closure models) or insufficient wake refinement (DDES, which ideally should switch to LES in the wake region). Moreover, more significant differences between each wake profile are observed in the DDES case, which might be caused by an average time window too small, considering that more turbulent content is resolved in relation to RANS. Indeed, a slice of the vorticity field, illustrated in Figure 7, shows a wake

with more vortices in the DDES case, more intense and longer convected.

6 PANS RESULTS

Now, the same simulations are performed for the intermediate grid G2, but using instead the PANS equations with three distinct f_k filters: 0.75, 0.50 and 0.25. The resulting integral forces are presented in Figure 8.

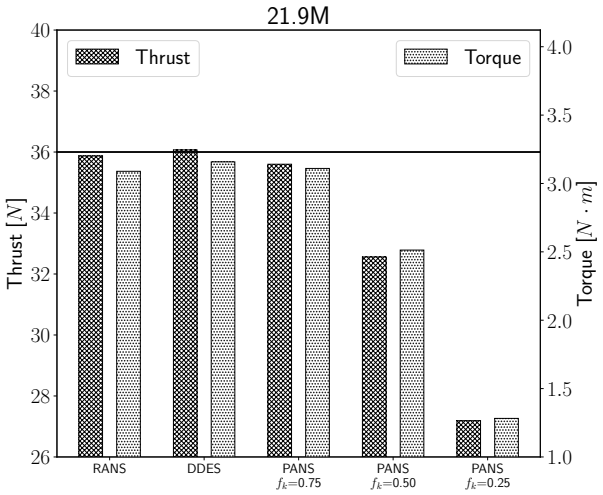

Figure 8: Integral forces obtained with RANS vs. DDES vs. PANS.

It is noticeable that as the PANS turbulence formulation is forced to resolve more turbulence scales ($f_k \rightarrow 0.0$), the integral forces reduce significantly and diverge from the experimental results. This phenomenon is explained by analysing the limiting streamlines on the surface of the blades in Figure 9. Since RANS models turbulence everywhere, it is able to predict a generally well attached flow with bi-dimensional features along the blade span with the exception of the root. The DDES formulation presents a very similar result, which is coherent considering that it contains a shielding function that forces always a fallback to RANS near the wall. Yet, with the PANS implementation used, the same filter f_k is applied everywhere in the domain, therefore part of the turbulent scales start to be resolved near the wall. This has an obvious impact on the flow features on the blade, with separation starting to occur earlier with $f_k = 0.75$ until the flow is completely separated with $f_k = 0.25$, which obviously impacts the integral forces.

Regarding the wake deficit, Figure 10 presents an improvement in the mixing region with $f_k = 0.25$ in relation to RANS and DDES - yet, since the flow is completely separated the cases are no longer comparable. In fact, the highly separated flow may be behind this improved mixing in conjunction with more turbulent content being actually resolved. In Figure 11 the spectral power content of a mid-radius cross-wire data point reflects precisely that. Whereas RANS presents the lowest turbulent energy content of all cases (all turbulent scales are modelled), increasing the f_k value of the filter is indeed contributing to more resolved turbulence in the simulation, even surpassing DDES with f_k equal to 0.50 and 0.25. Yet, all of the cases are still far from the turbulence content of the experiment, based on the cross-wire measurements provided. Moreover, frequencies higher than 10 Hz (smaller length scales) are apparently cut-off in the simulations. Therefore, most of the inertial subrange is simply not properly captured by the current simulations, which may be the cause of the differences observed in the wake deficit.

Based on the suggestion presented in [11], the minimum f_k value supported by the mesh is estimated based on a preliminary RANS simulation and Equation (9), as presented in Figure 12. It is clear from the white zones around the blades and immediately downstream of the rotor that even the finest grid, G3, presents a refinement level that is not able to support any kind of resolved turbulent length scale ($f_k > 1.0$).

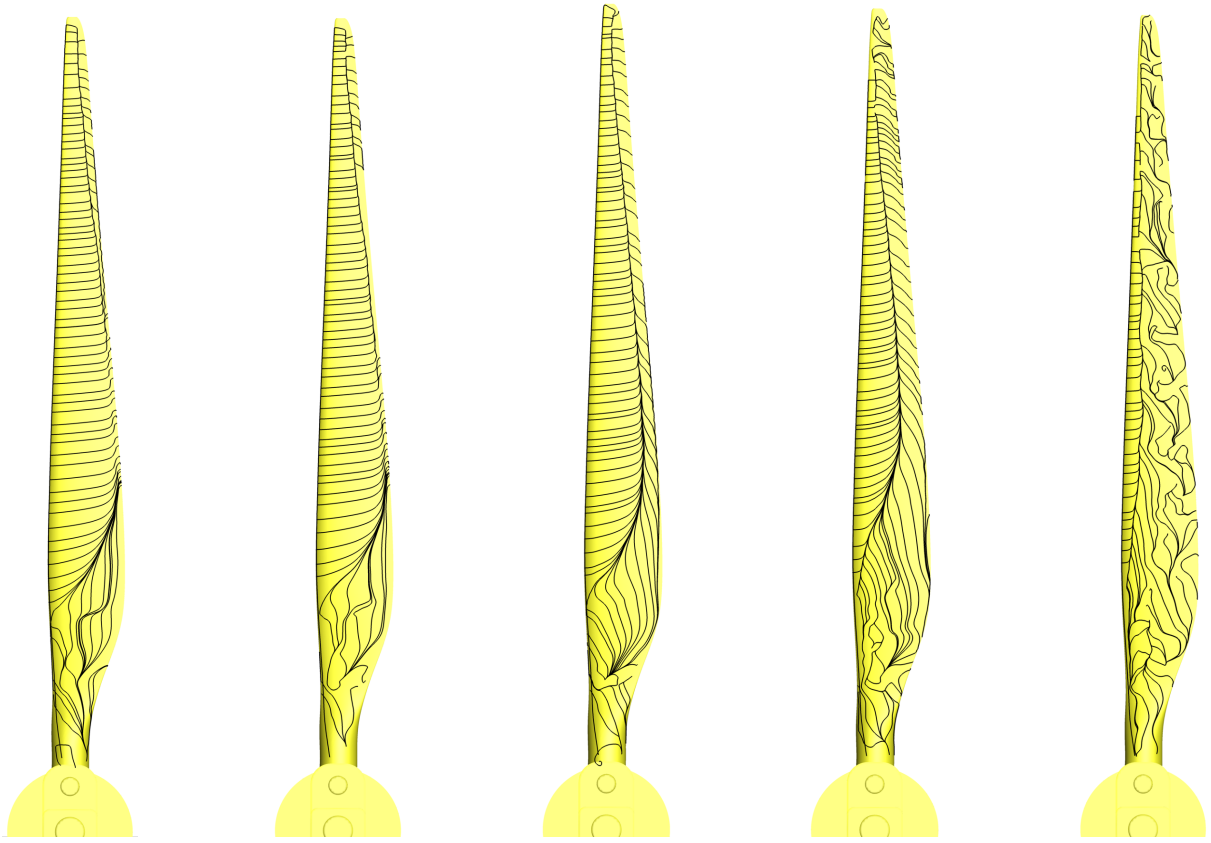

(a) RANS (b) DDES (c) $PANS_{75}$ (d) $PANS_{50}$ (e) $PANS_{25}$

Figure 9: Limiting streamlines on upper surface of a blade of the turbine.

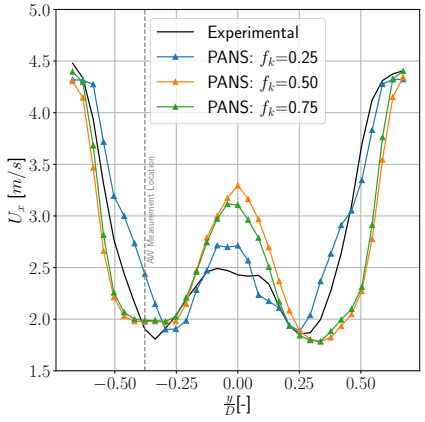

Figure 10: Average cross-wire velocity measurements $2.3D$ downstream.

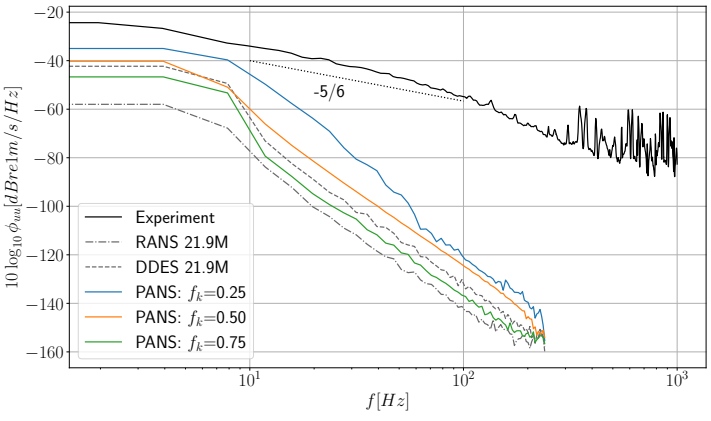

Figure 11: Axial velocity spectrum in cross-wire measurement located at the same y coordinate as the along-wire (AW) measurement.

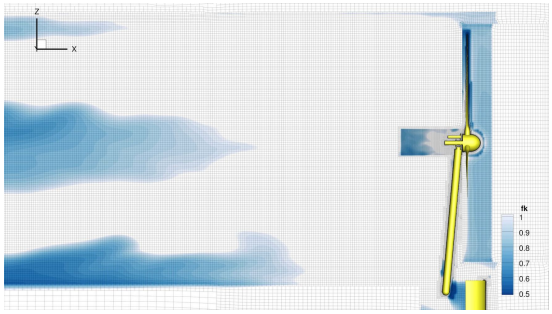

(a) Grid G1 (16.7M)

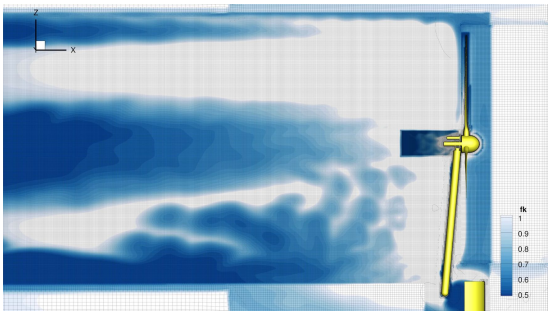

(b) Grid G3 (59.5M)

Figure 12: Minimum f_k supported by each mesh based on RANS and Eq. (9).

7 CONCLUSIONS

Both RANS and DDES approaches are suitable to predict the integral forces, as both model all turbulence scales near the wall. Yet, the two fail at capturing the wake mixing, which might be caused by a limitation of the models (in the case of RANS the $k-\omega$ SST closure model, which was not calibrated for wind turbine flows) and/or insufficient grid/time refinement. On the contrary, the PANS formulation used immediately fails at capturing the integral forces, especially at high ratios of resolved turbulence, f_k. This is caused by part of the turbulent scales being resolved nearby the wall, which are not supported by the mesh and impact the flow characteristics, including premature separation. In the literature it is suggested that PANS might suffer from this premature separation in relation to the experiments due to lack of turbulent content of the numerical inlet flow [10, 17] - the flow is laminar and is not able to transition, making it more prone to separation. As a workaround it is suggested the usage of synthetic turbulence generators together with finer grids [17].

From this exercise, it becomes obvious that the application of PANS is not as straightforward as RANS or DDES for such a practical application. This can be traced back to the filter f_k, which in this implementation is spatially constant. While this brings its own set of advantages in avoiding commutation errors [10], among these options DDES provides the best trade-off between simplicity and accuracy. Yet, future work should pursue synthetic turbulence generation, which might be the key to unlock improved results for this test case when using the PANS formulation.

8 ACKNOWLEDGMENTS

The authors acknowledge the usage of the HPC cluster Navigator, from the LAC laboratory of Universidade de Coimbra, under the project "Medium and High-fidelity Aerodynamic Models for Wind Farm Power Optimization" (2022.15647.CPCA.A2) funded by the FCCN. Part of the work was performed during the project "Floating Offshore Wind Modelling Cooperation" (FBR_OC2_49) funded by the Bilateral Relations Fund of the EEA Grants Portugal. The authors also thank Alessandro Fontanella for the UNAFLOW geometry and info on the experiment.

REFERENCES

[1] J. Steiner, R. P. Dwight, and A. Viré, "Data-driven RANS closures for wind turbine wakes under neutral conditions," *Computers & Fluids*, vol. 233, p. 105213, Jan. 2022.

[2] M. Baungaard, S. Wallin, M. P. Van Der Laan, and M. Kelly, "Wind turbine wake simulation with explicit algebraic Reynolds stress modeling," *Wind Energy Science*, vol. 7, pp. 1975–2002, Oct. 2022.

[3] C. Grinderslev, N. N. Sørensen, S. G. Horcas, N. Troldborg, and F. Zahle, "Wind turbines in atmospheric flow: fluid–structure interaction simulations with hybrid turbulence modeling," *Wind Energy Science*, vol. 6, pp. 627–643, May 2021.

[4] S. Heinz, J. Peinke, and B. Stoevesandt, "Cutting-edge turbulence simulation methods for wind energy and aerospace problems," *Fluids*, vol. 6, p. 288, Aug. 2021.

[5] S. S. Girimaji, "Partially-Averaged Navier-Stokes model for turbulence: A Reynolds-Averaged Navier-Stokes to Direct Numerical Simulation bridging method," *Journal of Applied Mechanics*, vol. 73, pp. 413–421, May 2006.

[6] J. O'Connor, S. Laizet, A. Wynn, W. Edeling, and P. V. Coveney, "Quantifying uncertainties in Direct Numerical Simulations of a turbulent channel flow," *Computers & Fluids*, vol. 268, p. 106108, Jan. 2024.

[7] F. R. Menter, M. Kuntz, and R. Langtry, "Ten years of industrial experience with the SST turbulence model," in *Turbulence, Heat and Mass Transfer 4*, Begell House, 2003.

[8] M. S. Gritskevich, A. V. Garbaruk, J. Schütze, and F. R. Menter, "Development of DDES and IDDES formulations for the k-ω Shear Stress Transport model," *Flow, Turbulence and Combustion*, vol. 88, pp. 431–449, Apr. 2012.

[9] F. S. Pereira, G. Vaz, and L. Eca, "An assessment of Scale-Resolving Simulation models for the flow around a circular cylinder," in *Proceeding of THMT-15. Proceedings of the Eighth International Symposium On Turbulence Heat and Mass Transfer*, (Sarajevo, Bosnia and Herzegovina), pp. 295–298, Begellhouse, 2015.

[10] F. S. Pereira, L. Eça, G. Vaz, and S. S. Girimaji, "Toward predictive RANS and SRS computations of turbulent external flows of practical interest," *Archives of Computational Methods in Engineering*, vol. 28, pp. 3953–4029, Aug. 2021.

[11] S. Girimaji and K. Abdol-Hamid, "Partially-Averaged Navier Stokes model for turbulence: implementation and validation," in *43rd AIAA Aerospace Sciences Meeting and Exhibit*, (Reno, Nevada), American Institute of Aeronautics and Astronautics, Jan. 2005.

[12] A. Fontanella, I. Bayati, R. Mikkelsen, M. Belloli, and A. Zasso, "UNAFLOW: A holistic wind tunnel experiment about the aerodynamic response of floating wind turbines under imposed surge motion," *Wind Energy Science*, vol. 6, pp. 1169–1190, Sept. 2021.

[13] G. Vaz, F. Jaouen, and M. Hoekstra, "Free-surface viscous flow computations: validation of URANS code FreSCo," in *Volume 5: Polar and Arctic Sciences and Technology; CFD and VIV*, (Honolulu, Hawaii, USA), pp. 425–437, ASMEDC, Jan. 2009.

[14] S. Lemaire and M. Klapwijk, "pyTST." Zenodo, Jan. 08, 2021. doi: 10.5281/zenodo.4428158.

[15] L. Eça, C. Klaij, G. Vaz, M. Hoekstra, and F. Pereira, "On code verification of RANS solvers," *Journal of Computational Physics*, vol. 310, pp. 418–439, Apr. 2016.

[16] L. Sileo, T. Gomes, V. Krasilnikov, and A. Maximiano, "Towards the CFD validation and analysis of aerodynamic loads acting on the rotor of a floating wind turbine subject to forced motions," in *Numerical Towing Tank Symposium (NuTTS2023)*, (Ericeira, Portugal), Oct. 2023.

[17] M. Klapwijk, T. Lloyd, G. Vaz, and T. van Terwisga, "On the use of synthetic inflow turbulence for Scale-Resolving Simulations of wetted and cavitating flows," *Ocean Engineering*, vol. 228, p. 108860, May 2021.